

Scoring the Impact of Unstructured Data Using Quantum Properties

Ying Zhao^{1[0000-0001-8350-4033]} and Charles C. Zhou^{2[0000-0001-9598-015X]}

¹ Naval Postgraduate School, Monterey, CA, 93943, USA

yzhao@nps.edu

² Quantum Intelligence, Inc., Prunedale, CA, 93907, USA

charles.zhou@quantumii.com

Abstract. A single collaborative and self-organizing agent (CSOA) represents a single system capable of ingesting local data and performing unsupervised machine learning and self-organization. Multiple CSOAs work collaboratively in a peer-to-peer network. Each agent has a peer list. Such multiple agents' collaboration can be modeled as cooperative games following quantum theories such as the quantum adiabatic evolution transformation (QAET), and quantum intelligence game (QIG) or the QAET-QIG framework. We first establish the theory of the QAET-QIG framework, and then apply it to predict the impact of the business news to companies' financial performance. The QAET-QIG framework achieves an accumulative 10% return where the market indexes are negative for a period of four months.

Keywords: quantum property · collaborative and self-organizing agents · CSOA · collaborative learning agents · CLA · quantum adiabatic evolution transformation · QAET · quantum intelligence game · QIG

1 Introduction

A single collaborative learning agent (CLA) [1, 2] ingests local data and performs data mining and machine learning. Multiple CLAs work collaboratively in a peer-to-peer network via a peer list. When we consider agent learning is unsupervised machine learning, CLAs are collaborative and self-organizing agents (CSOAs). We consider the CSOAs' interaction as an evolution process of quantum superpositions.

1.1 Quantum Evolution

A quantum evolution is modeled as a time-dependent quantum evolution characterized by Hamiltonians in Schrodinger's equations. Collaborative and self-organizing behavior of CSOAs in the process result in a total value of an agent with respect to its peer network. Equation (1) is the time-dependent Schrödinger equation and evolution of a quantum state $\psi(t)$:

$$i\hbar \frac{d}{dt} \psi(t) = H(t) \psi(t). \quad (1)$$

Equation (2) shows the solution to Equation (1):

$$\psi(t) = e^{-iH(t)t/\hbar}\psi(0) = U(t)\psi(0). \quad (2)$$

The operator $U(t) = e^{-iH(t)t/\hbar}$ is the time-evolution operator and unitary. The eigenstates of the Hamiltonian $H(t)$, known as energy eigenstates, are the solutions to the Schrödinger equation, form a complete basis set for the state space of the quantum system. A density matrix ρ of the wave function $\psi(t)$ is governed by the underlying $H(t)$. The evolution of ρ over time is determined by the energy eigenstates. Such an unsupervised learning system optimizes its value (e.g., energy or entropy) using natural mechanisms such as quantum adiabatic evolution transformation (QAET) [6]. According to the adiabatic theory, a QAET refers to a slow, continuous change of the Hamiltonian of a quantum system, where if the change is sufficiently slow or adiabatic, the system remains in its instantaneous ground state throughout the evolution. A QAET can play an essential role to generate more pure and entangled quantum states that are useful such as creating robust [7] topological orders for condensed materials.

In a traditional QAET setting [6], one assumes the beginning Hamiltonian is H_B and the ending Hamiltonian is H_C , the objective is to optimize the final measurement of $|\psi(T, \gamma, \beta)\rangle$ by changing $\gamma = (\gamma_1, \dots, \gamma_p)$ and $\beta = (\beta_1, \dots, \beta_p)$ in Equation (3) and Fig. 1 using hybrid classic and quantum computing to optimize parameters β_t and γ_t .

$$|\psi(T, \gamma, \beta)\rangle = \prod_{t=1}^T U_B(\beta_t) U_C(\gamma_t) |\psi(0)\rangle, \quad (3)$$

where

$$U_C(\gamma_t) = e^{-i\gamma_t H_C} \quad (4)$$

$$U_B(\beta_t) = e^{-i\beta_t H_B}. \quad (5)$$

In reality, external environment can change the Hamiltonian of a quantum system, for example, a measurement alters the system state based on the previous H_{t-1} 's eigenstate, collapses the system's wave function into the ground eigenstate. We show that such a measurement is accomplished by a quantum intelligence game (QIG) and forced by the environment.

1.2 Link to Knowledge Graphs

The knowledge graphs are embedded in the environment measurement of the Hamiltonian H . A team of CSOAs carry out a task with the following assumptions:

- The environment is modeled as the time-dependent Hamiltonian of a multi-agent system.
- When two capabilities are used together, the corresponding H graph might be directed, asymmetric, and causal, in other words, H might be non-Hermitian, which is different from the traditional quantum theory Hermitian matrix.

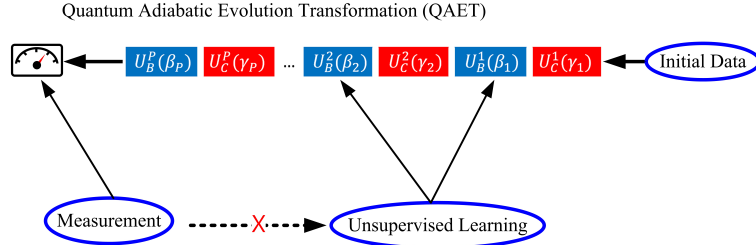


Fig. 1. Traditional quantum adiabatic evolution transformation (QAET): QAET needs a series of quantum unitary transformations using hybrid classic and quantum computing to optimize coherence parameters β_p and γ_p .

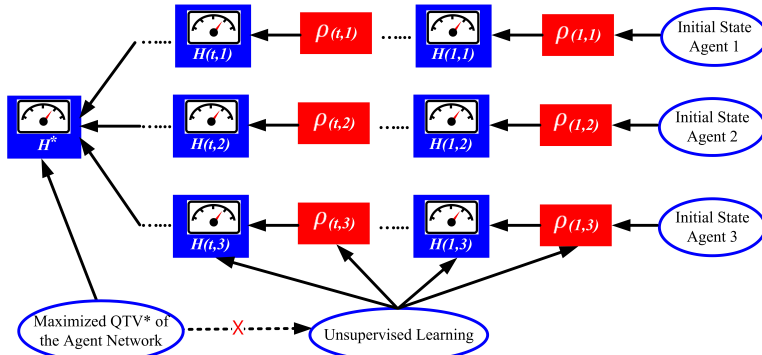


Fig. 2. Multi-Agent Collaboration. QAET-QIG : The value of a multi-agent system increases in a natural quantum mechanism QAET with repeated measurements in a QIG. The two processes are combined.

- Each agent does not have a full knowledge of the entire Hamiltonian and has to estimate from data-driven approaches learning from the environment shown in Fig. 2.

Such a graph-structured Hamiltonian measures causal relations between subcomponents and defines quantum states, linking to active research area of quantum causal models and quantum Bayesian networks. The contributions of this paper are summarized as follows:

1. We show that a multi-agent quantum system converges to an equilibrium state which has a high degree of purity and coherence via a QAET-QIG evolution. The convergence results in an equilibrium and measurable property or quantum theoretic value (QTV) of the system that is optimized. We demonstrate the QAET-QIG framework in Fig. 2, show one theorem, two unsupervised algorithms used to score new data for quantum values, and compare them with the traditional QAET (Fig. 1).
2. We apply the result to a use case to score quantum properties of financial news of about 9000 publicly traded companies in 2025. These quantum properties exhibit high correlation with observed dynamics.

2 Related Methods

2.1 Quantum Properties

In quantum mechanics, the state of a quantum system is described by a wave function ψ or, more generally, by a density matrix ρ . A density matrix is more insightful to describe if a quantum state is pure or mixed, if there are quantum coherence between states. Consider a multi-agent system behaves in a quantum sense, various quantum properties [9] can be computed.

- Purity: A pure state is a state that can be described by a single wave function. Equation (6) shows the purity caculation:

$$\text{Purity} = \sum_{k=0}^K \lambda_k^2, \quad (6)$$

where λ_k is the eigenvalues of the density matrix of a quantum system.

- Quantum entanglement entropy (QEE): QEE characterizes the randomness or disorder within a multi-agent system ρ . The eigenvalues $\lambda_k, k = 0, \dots, K$ of ρ , represent probabilities, so $\lambda_k > 0, k = 0, \dots, K$ and $\sum_{k=0}^K \lambda_k = 1$.

$$QEE = - \sum_{k=0}^K \lambda_k \ln(\lambda_k) \quad (7)$$

QEE for the whole system in a pure state (Purity = 1) is 0 according to Equation (7). QEE can be used to measure quantum topological phase transitions [13] or so called quantum topological order [5].

- Coherence: Coherence refers to the phases of quantum probability amplitudes and enables quantum superposition and interference. Coherence is measured using the L_1 norm of the off-diagonal elements of ρ as shown in Equation (8).

$$\text{Coherence} = \sum_{k \neq l} |\rho_{kl}| \quad (8)$$

2.2 Application of Perron-Frobenius Theorem and QAET

The Perron-Frobenius theorem [15] is primarily concerning non-negative matrices (i.e., matrices with all non-negative entries), or more specifically, irreducible non-negative matrices. Such a matrix has a unique largest positive eigenvalue, which is also the spectral radius of the matrix, the corresponding eigenvector has all its components positive for the largest eigenvalue. The eigenvalue is strictly larger in magnitude than all other eigenvalues. The Perron-Frobenius theorem provides the mathematical reasoning that a ground state exists when a wave function "collapses." If the operator of a measurement H is nonnegative and irreducible, the real eigenvalue corresponds to a state that remains physically measurable, while the other states corresponding to complex eigenvalues do not.

2.3 Game Theory: An Unsupervised and Self-Organizing Mechanism

The unsupervised and self-organizing mechanism, QAET-QIG, is achieved by an application of the Nash equilibrium (NE) [17]. In a classic or quantum game, NE characterizes a strategy ψ_l^* discourages a unilateral deviation such that

$$u_l(\psi_l^*) \geq u_l(\psi_l, \psi_{-l}^*) \quad (9)$$

for all ψ_l and l . (ψ_l, ψ_{-l}) is the choice of player l (self-player) relative to all other players $-l$ (opponent). u is a utility or measurement function.

3 Results

This section we present the main theorem of the paper.

Theorem 1 (QAET-QIG Evolves to a QTV). *A multi-agent system, with a Hamiltonian H environment measurement, which is assumed non-negative and irreducible, converges to an equilibrium state via a modified QAET process or a QAET-QIG process shown in Fig. 2. The evolution results in an equilibrium measurement. The quantum theoretic value (QTV) of the system is the equilibrium measurement or value in Equation (10) when $t \rightarrow \infty$. Each individual agent also reaches its own optimal value.*

$$QTV(t+1) = \langle \psi(t) | H(t+1) | \psi(t) \rangle \quad (10)$$

Proof. Consider a wave function of superposition in Equation (11):

$$|\psi(t)\rangle = \sum_{k=0}^K \sqrt{\lambda_k} e^{-i\frac{E_k t}{\hbar}} |\psi_k\rangle, \quad (11)$$

where E_k and $|\psi_k\rangle$, $k = 0, \dots, K$ are instantaneous eigenvalues and eigenvectors of $H(t)$, respectively. $|\psi_k\rangle$ can be functions of other attributes, e.g., X, Y, Z, omitted here for the proof, however, we give an example later showing this case.

$\lambda = \begin{bmatrix} \lambda_0 \\ \dots \\ \lambda_K \end{bmatrix}$, $\sum_{k=0}^K \lambda_k = 1$, and $\lambda_k > 0$ represent the probability amplitude of the superposition for time t . The density matrix is represented in Equation (12).

$$\begin{aligned} \rho(t) &= |\psi(t)\rangle \langle \psi(t)| \\ &= \begin{bmatrix} \lambda_0 & \sqrt{\lambda_0 \lambda_1} e^{-i(E_0 - E_1)t/\hbar} & \dots \\ \sqrt{\lambda_1 \lambda_0} e^{-i(E_1 - E_0)t/\hbar} & \lambda_1 & \dots \\ \dots & & \lambda_K \end{bmatrix} \end{aligned} \quad (12)$$

$\rho(t)$ is Hermitian: $\rho(t)^\dagger = \rho(t)$; idempotent: $\rho(t)^2 = (|\psi(t)\rangle \langle \psi(t)|)^2 = \rho(t)$, and Trace one: $\text{Tr}(\rho(t)) = \langle \psi(t) | \psi(t) \rangle = \sum_{k=0}^K \lambda_k = 1$. These properties imply that ρ has exactly one eigenvalue equal to 1, and all other eigenvalues are 0. So $\rho(t)$ is pure although it has multiple nonzero entries. In other words, $\psi(t)$ constructed in Equation (11) of a pure state of a complete coherent superposition.

$QTV(t+1)$ can be computed recursively. $|\psi(t)\rangle$ is measured on $H(t+1)$ where

$$H(t+1) = (V(t+1))^\dagger E(t+1) V(t+1) \quad (13)$$

is the eigenvalue decomposition of $H(t+1)$ with eigenvalues $E(t+1)$ and eigenstates $V(t+1)$. Let

$$|\psi'(t)\rangle = V(t+1) |\psi(t)\rangle, \quad (14)$$

Assume $H(t+1)$ is non-negative and irreducible, based on the Perron-Frobenius theorem, there is an unique real eigenvalue with the maximum magnitude, i.e., $|E_0(t+1)|$. $|E_0(t+1)| \geq |E_1(t+1)| \geq \dots \geq |E_K(t+1)| \geq 0$.

$$\begin{aligned} QTV(t+1) &= \\ &= \langle \psi(t) | H(t+1) | \psi(t) \rangle \\ &= \langle \psi(t) | (V(t+1))^\dagger E(t+1) V(t+1) | \psi(t) \rangle \\ &= \sum_{k=0}^K |E_k(t+1)| \langle \psi'_k(t) | \psi'_k(t) \rangle \\ &= \sum_{k=0}^K |E_k(t+1)| \lambda_k(t) \\ &\leq |E_0(t+1)| \end{aligned} \quad (15)$$

Equation (15) shows $QTV(t+1)$ is a weighted sum of eigenvalues of $H(t+1)$ and the weights $\boldsymbol{\lambda}(t) = \begin{bmatrix} \lambda_0(t) \\ \dots \\ \lambda_K(t) \end{bmatrix}$ are the probability amplitudes of the quantum state $|\psi(t)\rangle$ measured at the eigenstates $V(t+1)$ of $H(t+1)$.

In the QAET-QIG mechanism, in addition to the superposition Equation (11) that is critical, the quantum effect is further reinforced by using a QIG. We assume each quantum agent l tries to change the quantum configuration component of itself $\boldsymbol{\lambda}$ to increase its own value. Each agent's value is λ_l . According to the notation in Equation (9), $\boldsymbol{\lambda}$ is the quantum superposition state in Equation (11): Given the rest of the agents' state is $\psi_{-l}(\boldsymbol{\lambda})$ and value is $\lambda_{-l}(\boldsymbol{\lambda})$, ψ_l can be only $\psi_l(\boldsymbol{\lambda})$ because the parts of a pure state are not independent, they "move" or behave like a single, inseparable whole.

$$\lambda_l + \lambda_{-l} = 1. \quad (16)$$

In realistic quantum processes, the H is often not known in advance, it acts on the quantum state $|\psi\rangle$, the system undergoes a collapse with a probability λ_l . This means that components of $|\psi\rangle$ which better align with the dominant eigenvectors of H are more likely to survive measurement.

■

Consider $K = 1$ in Equation (11), ψ_0 and ψ_1 are two orthogonal circles for data attributes such as locations (X, Y, Z). Super-positioning the ψ_0 and ψ_1 with parameters $\hbar = 1.0$.

$$\psi(X, Y, Z, t) = \sqrt{\lambda_0} e^{-iE_0 t} \psi_0(X, Y, Z) + \sqrt{\lambda_1} e^{-iE_1 t} \psi_1(X, Y, Z) \quad (17)$$

represents a quantum point in the three dimensional space evolves according to Equation (18), a torus in Fig. 3 as a result of a superposition and evolution of two eigen-states. Fig. 4 shows the probability amplitude in the torus.

$$\begin{aligned} X &= (R + r \cos(\theta(t))) \cos(\phi(t)) \\ Y &= (R + r \cos(\theta(t))) \sin(\phi(t)) \\ Z &= r \sin(\theta(t)) \end{aligned} \quad (18)$$

$$R = \lambda_0 + \lambda_1 = 1 \quad (29)$$

$$r = 2\sqrt{\lambda_0 \lambda_1} \quad (30)$$

$$\theta(t) = E_0 t \quad (31)$$

$$\phi(t) = E_1 t \quad (32)$$

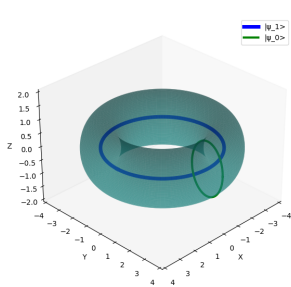


Fig. 3. A Torus as a Result of a Superposition and Evolution of Two Eigenstates

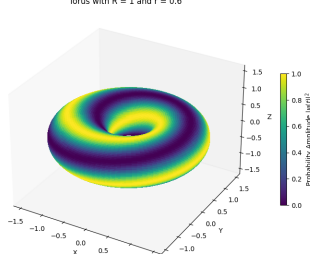


Fig. 4. Probability Amplitudes of a Quantum State on the Torus Formed by Superpositioning Two Orthogonal Eigenstates as Bases

3.1 Scoring a Quantum State on Rank-1 Measurement H

Given a quantum state constrained to the torus-evolving form:

$$\psi(t) = \sqrt{\lambda_0} e^{-iE_0 t} \psi_0 + \sqrt{\lambda_1} e^{-iE_1 t} \psi_1, \quad (19)$$

where ψ_0, ψ_1 are orthonormal, and $\lambda_0 + \lambda_1 = 1$. We are considering a parametric measurement operator H :

$$H(\alpha) = \begin{bmatrix} \cos^2 \alpha & \cos \alpha \sin \alpha \\ \cos \alpha \sin \alpha & \sin^2 \alpha \end{bmatrix} = |\phi\rangle\langle\phi|, \quad \text{where } |\phi\rangle = \begin{bmatrix} \cos \alpha \\ \sin \alpha \end{bmatrix}. \quad (20)$$

This is a rank-1 projector since the maximum eigenvalue is 1. This expression is maximized when $\begin{bmatrix} \lambda_0 \\ \lambda_1 \end{bmatrix} = \begin{bmatrix} \cos \alpha \\ \sin \alpha \end{bmatrix}$. In other words, when the state aligns the best to the top eigen vector of the measurement H . We have

$$QTV_{max_rank-1} = \max_t \langle \psi(t) | H(\alpha) | \psi(t) \rangle = (\cos \alpha \sqrt{(1 - \lambda_1)} + \sin \alpha \sqrt{\lambda_1})^2 = 1.$$

(21)

3.2 Scoring a Quantum State on Any H

For any given measurement operator H with real matrix elements:

$$a = \langle \psi_0 | H | \psi_0 \rangle, \quad b = \langle \psi_1 | H | \psi_1 \rangle, \quad c = \langle \psi_1 | H | \psi_0 \rangle, \quad d = \langle \psi_0 | H | \psi_1 \rangle, \quad (22)$$

or

$$H = \begin{bmatrix} a & c \\ d & b \end{bmatrix} = \begin{bmatrix} \langle \psi_0 | H | \psi_0 \rangle & \langle \psi_0 | H | \psi_1 \rangle \\ \langle \psi_1 | H | \psi_0 \rangle & \langle \psi_1 | H | \psi_1 \rangle \end{bmatrix} \quad (23)$$

The instantaneous measurement value $\psi(t)$ on H is:

$$QTV(t, \lambda_1) = a\lambda_0 + b\lambda_1 + \sqrt{\lambda_0\lambda_1} (c e^{i\Delta t} + d e^{-i\Delta t}), \quad \text{where } \Delta = E_0 - E_1 \quad (24)$$

This value is not necessarily real unless:

$$c e^{i\Delta t} + d e^{-i\Delta t} \in \mathbb{R}$$

This is maximized when:

$$\cos(\Delta t) = 1 \quad \Rightarrow \quad \Delta t = 2\pi n, \quad n \in \mathbb{Z}$$

$$QTV_{max_coherent}(\lambda_1) = \max_t \langle \psi(t) | H | \psi(t) \rangle = (1 - \lambda_1)a + \lambda_1 b + (c + d)\sqrt{(1 - \lambda_1)\lambda_1}. \quad (25)$$

The coherence value arises from the *superposition* structure of the state and the measurement operator H . Rank-1 projective measurement is not always optimal in Equation (21), because $QTV_{max_coherent}(t) = \langle \psi(t) | H | \psi(t) \rangle > 1$, when $|c| > 0.5$, we have $\lambda_{\max}(H) > 1$.

3.3 Classical State with Quantum Measurement

Let the system be described by an incoherent mixture (a classical probability distribution over orthogonal states):

$$\rho = (1 - \lambda_1)|\psi_0\rangle\langle\psi_0| + \lambda_1|\psi_1\rangle\langle\psi_1|. \quad (26)$$

Now consider the same measurement H with off-diagonal components:

$$H = \begin{bmatrix} a & c \\ d & b \end{bmatrix} \quad \text{in basis } \{\psi_0, \psi_1\}. \quad (27)$$

The expectation value of the measurement such a quantum system is:

$$QTV_{max_mixed} = \langle H \rangle = \text{Tr}(\rho H) = (1 - \lambda_1)a + \lambda_1 b. \quad (28)$$

Equation (25) can optimizes QTV depending on the interplay of the parameters λ_1, a, b, c .

Fig. 5 shows a comparison of the measurement of a quantum state measurement on Rank-1 Projector (blue): $H_\alpha = |\phi(\alpha)\rangle\langle\phi(\alpha)|$ with $\alpha = \frac{\pi}{8}$, capturing coherent superposition but bounded by 1; and the one on a coherence (dashed red): $H = \begin{bmatrix} a & c \\ \bar{c} & b \end{bmatrix}$ with $a = 0.85, b = 0.15, |c| = 0.8$. This measurement fully utilizes coherence and yields the highest output, $QTV_{max} \approx 1.3732$ at $\lambda_1^* \approx 0.299$; and a mixed State (gray dotted): A classical mixture without coherence, yielding a linear response.

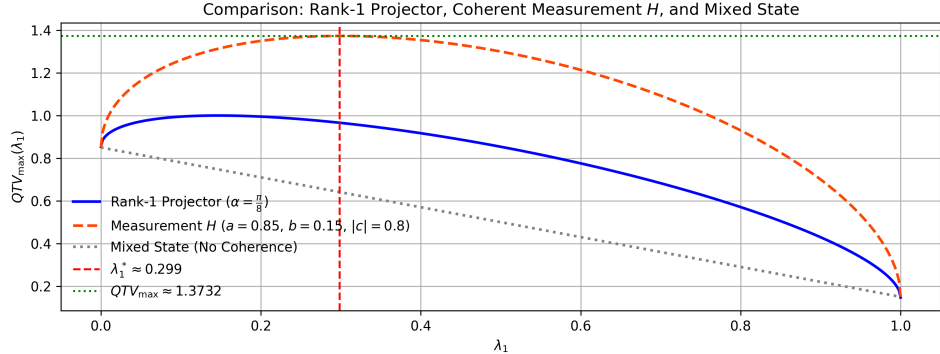


Fig. 5. Comparison of Measurement Strategies

4 Algorithms Using the QAET-QIG Framework

The algorithms shown below provide screening and scoring methods to evaluate information fusion that favor quantum effects.

4.1 Rank-1 Projective Measurement

We create a quantum control loop in quantum space as shown in Algorithm 1. $|E_0(t+1)| \geq |E_0(t)|$ can only be achieved via the QAET process combined with the QIG process because otherwise the agents would not have incentives to move around. Each agent and the entire system (i.e., the social welfare) both encapsulate the optimal values. The Perron-Frobenius theorem specifies the condition for $H(t)$ to have at least one real positive maximum eigenvalue that serves the maximum QTV and the corresponding eigenvector serves as the quantum measurement for each agent component. Each agent does not have a full knowledge of the entire Hamiltonian and has to estimate from data-driven approaches as shown in Fig. 2.

4.2 Coherence Exploitation

A CSOA quantum system can start with two orthogonal states, each agent represents semantically distinct contents, when measured appropriately, can evolve and give rise to higher value.

For multiple CSOAs, we first divide observable variables such as words or concepts in all CSOAs' content into patterned (P) themes, emerging (E) themes, and anomalous (A) themes using a community detection algorithm [16].

- Patterned (P) themes: A patterned theme is more likely to be shared across multiple diversified domains, which are already in the public consensus and awareness and can be authoritative to define values.

Algorithm 1 Quantum Property Scoring Algorithm - Rank-1 Projection

```

while  $t \geq 0$  do
    Compute the eigen-state  $V_{H_0}(t)$  of  $H(t)$  corresponding to its largest real eigenvalue
     $|E_{H_0}(t)|$ 
    for Each quantum state  $\lambda(t-1) = \begin{bmatrix} \lambda_0(t-1) \\ \dots \\ \lambda_K(t-1) \end{bmatrix}$  of a collaborative learning agent
         $i$  do
            Measure the projection  $S_i(t) = \lambda(t-1)^T V_{H_0}(t)$  as the score
        end for
        Sort and output  $S(t)$ 
        Update  $\lambda(t) = S(t)$ 
        Estimate new  $H(t+1)$ 
    end while

```

- Emerging (E) themes: These themes tend to become patterned over time.
- Anomalous (A) themes: These themes may not seem to belong to the data domain as compared to others. They can be interesting, unique, innovative to specific entities and may be high-value and need further investigation.

P and A are semantically different and can serve as two orthogonal bases for superpositions in this study. We apply such a quantum superposition of P and A as an information fusion by coherent exploitation [3] in our use case.

Let the value of a content ct computed from patterned (P) themes be $P(t, j, ct)$ and from anomalous (A) themes be $A(t, j, ct)$ for Agent j at time t , respectively. Each Agent j fuses all the models from its peer agents [16]. The total value $V(t, j, ct)$ for ct is a function of $P(t, j, ct)$ and $A(t, j, ct)$ as shown in Eq. (29).

$$V(t, j, ct) = f(P(t, j, ct), A(t, j, ct)). \quad (29)$$

In this model, the quantum state represents a superposition of P and A :

$$|\psi\rangle = \sqrt{\lambda_0} e^{-iE_0 t} |P\rangle + \sqrt{\lambda_1} e^{-iE_1 t} |A\rangle, \quad (30)$$

and $\lambda_0 + \lambda_1 = 1$. This framework allows for the modeling of coherence between P and A which create extra value. λ_0 and λ_1 presents a degree of a state in each component. $V(t, j, ct)$ are estimated using Algorithm 1 and Algorithm 2, and compared with other unsupervised machine learning methods.

5 Use Cases

The QAET-QIG theory has many applications such as scoring quantum properties for condensed materials, and hybrid force [18] in defense industry. Here we focus on an open source data application of the impact (QTV) of daily business news.

The business news of a publicly traded company can either positively or negatively impact stock prices in the following days. The impact of a business

Algorithm 2 Quantum Property Scoring Algorithm - Coherence Exploitation

```

while  $t \geq 0$  do
    for each Agent  $j$  do
        Separate popular and anomalous content into  $[\mathbf{P}(t, j), \mathbf{A}(t, j)]$ 
    end for
    for each content  $ct$  of Agent  $j$  do
         $V(t, j, ct) \leftarrow \left[1 + \frac{A(t, j, ct)}{L}\right]^{\frac{P(t, j, ct)}{L}}$ 
    end for
end while

```

news is modeled as a QTV in the use case. Each company is a content provider and self-player, and its news audience or Market is the opponent. Daily business news content, collected from January 5th, 2025 to April 24th, 2025 of 75 trading days for more than 9000 publicly traded companies. The use case was used to validate quantum scoring algorithms.

For each day, the total news for all the companies was analyzed daily, then the models are used to score each stock with the starting price $> \$5$ and market value $> \$1 billion$ compared with various other unsupervised machine learning methods to predict the next day return R_{t+1} . The ground truth of R_{t+1} were extracted from actual returns in the next day. For example, in Fig. 6, SPY-01-05-2025 shows company SPY selected because it has the highest score using the Coherent method for 01-05-2025, the return was computed for the next day 01-06-2025:

$$\text{Ground Truth QTV} = \text{Daily Return}(DR) = \frac{\text{Close} - \text{Open}}{\text{Open}} \quad (31)$$

Keywords from business news are different among different industries and changing dynamically over time. Traditional supervised machine learning and predictive algorithms are difficult to apply successfully. We first apply the CSOA to the whole day's news for Day t and discover patterned, emerging, and anomalous themes. We then apply Algorithm 1, Algorithm 2, to score each news for each company for Day t . We finally sort and rank the news and companies according to each algorithm, select the top-scored company according to each algorithm. Finally, we compute the daily return Day $t + 1$ for the selected company using Equation (31). We finally compare the total returns for 75 trading days for the methods listed.

Unsupervised machine learning algorithms of the following were used on the data set:

1. Coherent: Algorithm 2
2. Rank-1: Algorithm 1
3. Sentiment Low: Select the top-scored company using the descending sentiment
4. Sentiment High: Select the top-scored company using the ascending sentiment

5. QQQ: One of the index ticker and daily returns
6. SPY: One of the index ticker and daily returns
7. DDM: One of the index ticker and daily returns

Fig. 6 shows daily company selections using different algorithms. Fig. 7 shows a comparison of news impact using different algorithms.

Coherent		Rank-1		Sentiment Low		Sentiment High		QQQ	SPY	DDM
Selection	Return	Selection	Return	Selection	Return	Selection	Return	Return	Return	Return
SPY-01-05-2025	-0.0015	AEP-01-05-2025	-0.0188	TMUS-01-05-2025	-0.0050	ALL-01-05-2025	-0.0298	0.0010	-0.0081	-0.0080
ING-01-06-2025	-0.0063	HPQ-01-06-2025	-0.0103	PANW-01-06-2025	-0.0113	LUV-01-06-2025	-0.0315	-0.0198	0.0075	-0.0167
CART-01-07-2025	-0.0031	PLTR-01-07-2025	0.0016	ASO-01-07-2025	0.0361	MMS-01-07-2025	0.0090	0.0004	-0.0015	0.0039
CMA-01-09-2025	-0.0131	AXTA-01-09-2025	0.0036	AMC-01-09-2025	-0.0256	AIZ-01-09-2025	-0.0176	-0.0084	-0.0147	-0.0233
LYFT-01-12-2025	0.0156	AUR-01-12-2025	-0.0725	KEYS-01-12-2025	0.0097	TAL-01-12-2025	0.0185	0.0087	0.0013	0.0199
BURL-01-13-2025	-0.0109	GDDY-01-13-2025	0.0106	INVH-01-13-2025	-0.0003	RCL-01-13-2025	0.0003	-0.0072	-0.0092	0.0014
BKR-01-14-2025	0.0022	JPM-01-14-2025	0.0078	BOKF-01-14-2025	-0.0086	PFGC-01-14-2025	-0.0066	0.0072	0.0098	0.0030
FSLY-01-15-2025	0.0161	BKH-01-15-2025	0.0370	LMT-01-15-2025	0.0105	AFRM-01-15-2025	-0.0159	-0.0114	-0.0037	-0.0027
TRV-01-16-2025	-0.0111	DKNG-01-16-2025	-0.0192	EXAS-01-16-2025	0.0187	PLMR-01-16-2025	0.0101	-0.0021	0.0042	0.0008
INDV-01-20-2025	-0.0008	DJT-01-20-2025	-0.0532	AU-01-20-2025	0.0014	VNO-01-20-2025	0.0012	0.0006	-0.0043	0.0174
GSK-01-21-2025	-0.0062	BK-01-21-2025	-0.0054	JBHT-01-21-2025	0.0083	BR-01-21-2025	0.0056	0.0037	0.0010	-0.0004
GTX-01-22-2025	0.0138	AAL-01-22-2025	-0.0156	WLFC-01-22-2025	0.0137	AGI-01-22-2025	0.0060	0.0068	0.0040	0.0175
HWM-01-23-2025	0.0002	SF-01-23-2025	0.0025	ENB-01-23-2025	0.0029	C-01-23-2025	-0.0001	-0.0064	0.0009	-0.0033
TTD-01-26-2025	0.0180	SAIA-01-26-2025	0.0165	NUE-01-26-2025	-0.0059	CCL-01-26-2025	0.0268	0.0063	0.0065	0.0303
...										
...										
Sum	0.1003		-0.4211		-0.0758		-0.0875	-0.0985	0.0294	-0.1471

Fig. 6. Daily Company Selections Using Different Algorithms

The rank-1 value change is instant when a quantum state is aligned with the measurement H 's top eigen-state as shown in Equation (21), while the coherence-enhanced value is time-dependent according to Equation (25). So the value oscillates over time due to interference. The maximum measurement only occurs periodically. If a quantum state is well-aligned, then a rank-1 value gives the maximum possible measurement immediately. It is sharp, local, and needs no dynamics or it "collapses" to the maximum eigen-state instantly. However, the rank-1 is not always better: If the quantum state is not aligned, rank-1 gives low signal. The rank-1 measurement does not require communication between eigen states. It only responds at the moment of measurement. On the contrary, the coherent measurement requires knowledge of global phase and evolution over time. The coherent value oscillates, reaching peaks only at moments of the constructive interference that enhances the total measurement value. Consequently, the news' impact (-0.4211) peaks fast before the start of the next day trading using the Rank-1 algorithm, compared to the Coherent Algorithm (0.1003), which peaks during the next trading day.

However, interference isn't always constructive to enhance the total measurement value, so synergy isn't guaranteed — it depends on phase alignment. This gives quantum theory a richer landscape than classical synergy.

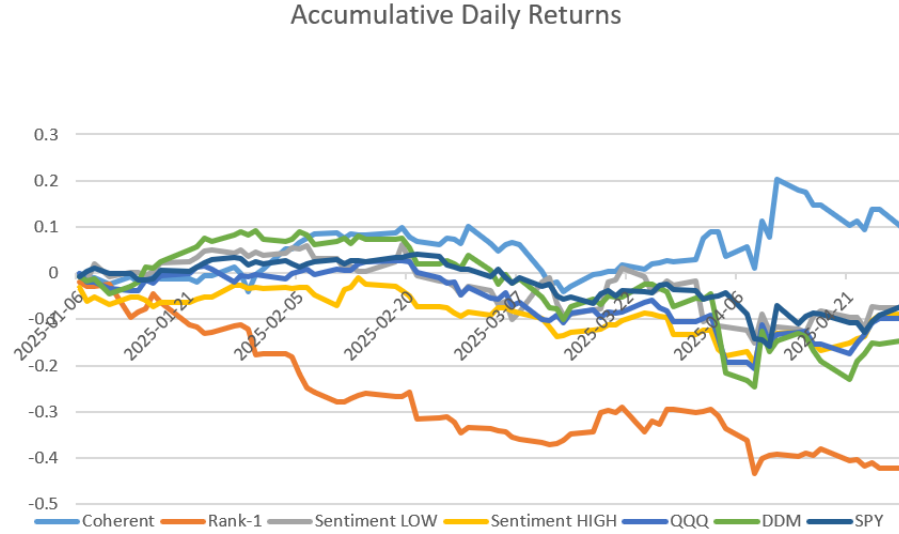


Fig. 7. Comparison of News Impacts Using Different Algorithms

6 Conclusion

In this paper, we show a new QAET-QIG framework, where a repeated measurement forced by the environment with CSOAs in a QAET process. We also show a QIG process is essential for the QAET process to converge and "collapse" to good measurement values.

Acknowledgment

The views and conclusions contained in this document are those of the authors and should not be interpreted as others or representing the official policies, either expressed or implied of the U.S. Government.

References

1. Zhou, C., Zhao, Y., & Kotak, C. (2009). The Collaborative Learning agent (CLA) in Trident Warrior 08 exercise. In Proceedings of the International Conference on Knowledge Discovery and Information Retrieval - Volume 1: KDIR, IC3K (pp. 323-328) DOI: 10.5220/0002332903230328. Madeira, Portugal.
2. Zhao, Y., & Zhou, C. (2023). Quantum Theoretic Values of Collaborative and Self-organizing Agents. ASONAM '23: Proceedings of the 2023 IEEE/ACM International Conference on Advances in Social Networks Analysis and Mining November 2023. Pages 678-685. Kusadasi, Turkiye, November 6 - 9, 2023. <https://dl.acm.org/doi/10.1145/3625007.3627509>

3. Zhou, C. C. & Zhao, Y. (2023). Crowd-Sourcing High-Value Information via Quantum Intelligence Game. In: Arai, K. (eds) Intelligent Computing. SAI 2023. Lecture Notes in Networks and Systems, vol 711. Springer, Cham. https://doi.org/10.1007/978-3-031-37717-4_34.
4. Zhao, Y., Mata, G. & Zhou, C. (2023). Self-organizing and Load-Balancing via Quantum Intelligence Game for Peer-to-Peer Collaborative Learning Agents and Flexible Organizational Structures. In: Arai, K. (eds) Intelligent Computing. SAI 2023. Lecture Notes in Networks and Systems, vol 711. Springer, Cham. https://link.springer.com/chapter/10.1007/978-3-031-37717-4_33
5. Wen, Xiao-Gang (1990). Topological Orders in Rigid States. *Int. J. Mod. Phys. B.* 4 (2): 239. doi:10.1142/S0217979290000139.
6. Farhi, E., Goldstone, J., & Gutmann, S. (2014). A Quantum Approximate Optimization Algorithm, arXiv Prepr. arXiv1411.4028, pages 1-16, 2014.
7. S. Dusuel, M. Kamfor, R. Orus, K. P. Schmidt, J. Vidal (2011). Robustness of a perturbed topological phase. <https://arxiv.org/abs/1012.1740>
8. Yingwen Zhang, Dao-Xin Yao, and Zhi Wang (2023). Topological superconductivity with large Chern numbers in a ferromagnetic-metal–superconductor heterostructure. *Phys. Rev. B* 108, 224513 – Published 18 December 2023
9. John von Neumann, J. (1955). Mathematical Foundations of Quantum Mechanics. Princeton University Press. ISBN 978-0-691-02893-4.
10. Barile, M. & Weisstein, E. W. (2023). Betti Number." <https://mathworld.wolfram.com/BettiNumber.html>
11. Che, Y., Gneiting, C., T Liu, T. & Nori, F. (2020). Topological quantum phase transitions retrieved through unsupervised machine learning. *Physical Review B*, 2020.<https://arxiv.org/pdf/2002.02363.pdf>
12. Continentino, M. (2017). Quantum Scaling in multi-agent Systems – An Approach to Quantum Phase Transitions. Cambridge University Press.
13. Kartik, Y. R. Kumar, R.R. & Sarkar, S. (2020). Topological Quantum Phase Transitions and Criticality in a Longer-Range Interacting Kitaev Chain. *Physical review B* 9 September 2020.
14. Hofstadter, D. (2004). Teuscher, C. (ed.). Alan Turing: Life and Legacy of a Great Thinker. Springer. p. 54. ISBN 978-3-540-20020-8.
15. Meyer C. D.(2000), Matrix Analysis and Applied Linear Algebra. SIAM, ISBN 978-0-89871-454-8
16. Newman, M. E. J. (2006). Finding community structure in networks using the eigenvectors of matrices. *Phys. Rev. E* 74, 036104.
17. Lotidis, K., Mertikopoulos, P., and Bambos, N. (2023). Learning in Quantum Games.
18. Zhao, Y. (2024). Quantum Theoretic Values of Collaborative and Self-Organizing Agents in Forming a Hybrid Force. In the 29th ICCRTS Proceedings, 24-26 September 2024 · London, UK.